Eur. Phys. J. B **46**, 335–342 (2005)
DOI: 10.1140/epjb/e2005-00258-4

THE EUROPEAN PHYSICAL JOURNAL B

Heating of condensation surface during magnetron sputtering

L.R. Shaginyan[1,a], V.R. Shaginyan[2], and J.G. Han[3]

[1] Institute for Materials Science Problems of National Academy of Sciences of Ukraine, Krzhizhanovsky str., 3, Kiev-03142, Ukraine
[2] Petersburg Nuclear Physics Institute, Gatchina, 188300, Russia
[3] Center for Advanced Plasma Surface Technology, Sungkyunkwan University 300 Chun-Chun-Dong Jangan-gu Suwon, 440-746 Korea

Received 7 December 2004 / Received in final form 31 March 2005
Published online 18 August 2005 –

Abstract. Chromium films deposited by magnetron sputtering on non-heated substrates from non-thermalized atoms crystallize in regular bcc Cr phase, with non-uniform microstructure and lattice constant along the thickness. These non-uniformities decrease with elevation of the substrate temperature and vanish at a certain value. However films deposited on non-heated substrates from thermalized atoms crystallize in a low-temperature Cr phase and have almost uniform microstructure. We have developed a model explaining this effect, which is based on the supposition of the formation of a "hot" layer on the growth surface during deposition, whose temperature depends on the flux of energy delivered to the condensation surface and can be noticeably higher than the substrate temperature. Detailed investigation of the structure of Cr films deposited at various temperatures and energy fluxes delivered to the growth surface, correlate well with the above model.

PACS. 68.35.Ja Surface and interface dynamics and vibrations – 68.37.Lp Transmission electron microscopy (TEM) (including STEM, HRTEM, etc.)

1 Introduction

A key parameter that defines the structure of a film is the temperature at which the film forms. In our previous investigation it was shown that Cr films deposited by magnetron sputtering on non-heated substrates have non-uniform crystal structure and microstructure along the thickness. The lattice parameter in the film region adjacent to the substrate is noticeably larger than the equilibrium value, and crystallites forming in this region are small. As the film growth proceeds the lattice parameter decreases towards the equilibrium value and the crystallite size increases. It was supposed that the reason for this effect is the gradually increasing difference between the temperature on the condensation surface and the conventional substrate temperature during the film deposition [1].

In this paper, we present additional experimental results and a theoretical model demonstrating that the temperature gradually increases within a thin surface layer of the growing film during deposition. At a certain moment it reaches a value substantially higher than the conventional substrate temperature. Following the well known concept explaining that the substrate temperature rise during magnetron sputtering is a result of the energy delivered to the substrate surface by sputtered atoms and from the plasma [2,3] we prove however that this temperature is non-uniformly distributed along the substrate and achieves a maximum value at the condensation surface.

2 Experimental details

Cr films were deposited on single crystal silicon wafers by the balanced magnetron sputtering of a Cr target with a diameter of 50 mm in argon plasma. The substrate holder was equipped with a chromel-alumel thermocouple mechanically attached to the holder using silver paste for better thermal contact. The base pressure in the chamber (volume $\sim$ 0.7 m^3) was around $(1-2)\times10^{-3}$ Pa. The fixed deposition parameters were: the discharge current $I_d = 0.4$ A, the substrate-to-target distance 50 mm, while variables were the Ar pressure, $P_{\rm Ar}$, and the substrate temperature, T_s. The target voltage was dependent on $P_{\rm Ar}$ and was $\sim$–450 V for $P_{\rm Ar} = 5$ Pa and $\sim$–500 V for $P_{\rm Ar} = 0.2$ Pa. The substrate was either not heated, or heated up to a specified temperature before deposition using resistance heating. The negative floating potential developed on the substrate holder during deposition was between -12 and -14 V for $P_{\rm Ar} = 0.2$ Pa and around -6 V for $P_{\rm Ar} = 5$ Pa pressures. A 15 min pre-sputtering of the target before actual deposition provided stable deposition conditions, including the working and residual gas

[a] e-mail: shagin@skku.edu

pressures. The film thickness was in the range 1–6 μm and the deposition rate was in the range of 4–5 nm/s depending on the deposition conditions.

The cross-sections of Cr films for structure investigations were prepared by a two-step procedure including mechanical polishing and subsequent ion milling. The structure of three parts of the samples (lower part of the film adjacent to the substrate, middle and upper parts of the film) was analyzed using selected area electron diffraction (SAED) and high-resolution transmission electron microscopy (HRTEM). For this purpose a high-resolution (0.2 nm by point, 300 kV accelerating voltage) electron microscope JEOL-3010 was utilized. The diameter of the selected area on the sample was about 0.2 μm. Special measures were taken to increase the accuracy of the lattice parameter a measurements from SAED data. At first, SAED patterns from different parts of the film were taken along with a SAED pattern from a silicon substrate, which served as a built-in-standard for accurate measurement of a camera constant. Secondly, the lattice parameters for each film part were calculated as average values of all interplanar distances available from SAED pattern taken from this film part, and which are given in Table 1 along with the standard deviations. The composition of films deposited on non-heated substrates both in low- and high-pressure conditions was studied by energy dispersive X-ray (EDX) analysis using an EDX spectrometer (energy resolution 138 eV, spatial resolution 10 nm) attached to the scanning electron microscope, S3500H. The analysis has shown that the films contained only chromium and 1.3–1.5 weight % of carbon without any traces of oxygen and argon.

To verify the influence of the energy input to the condensation surface delivered by atoms and from the plasma on the growth temperature, Cr films were deposited at two values of Ar pressure: $P_{\mathrm{Ar}} = 5$ Pa (high-pressure conditions) and 0.2 Pa (low-pressure conditions). To be sure that the film has actually grown at the lowest substrate temperature (i.e., from fully thermalized atoms and minimal plasma influence) the film has been deposited on the backside of a free-hanging Si wafer. For this purpose, the wafer has been suspended with the help of a special holder instead of the usually used substrate holder so that the film could be deposited on both sides of the substrate. In this case, the film formed on the backside of the substrate has been deposited from flux of fully thermalized Cr atoms [4]. Measurements of the temperature developed on the backside of the substrate have shown that the temperature did not exceed ∼75°C.

3 Results

3.1 Films deposited from low-energy atomic fluxes (high-pressure conditions)

Cell parameters calculated from ring SAED patterns taken from different parts of the film deposited under such conditions are presented in Table 1. Comparison of experimentally measured interplanar distances and corresponding calculated lattice parameters, with those given in [5] shows that the film grown at high-pressure conditions crystallized in the low-temperature (LT) Cr phase. Along with lines from the LT Cr phase in the upper part of this film there are also two very weak lines, which can be attributed to the ordinary bcc high-temperature (HT) Cr phase. Note that the LT Cr phase exists at temperatures below 400 °C and rapidly transforms into bcc HT phase at temperatures above 450 °C [5]. A small increase in a lattice parameter of order 0.2% in the upper part of the film compared to the lower part is seen from Table 1.

The microstructure of the majority of this film is uniform and consists of narrow columns with average diameter 90 nm (Fig. 1a). The average crystallite size is from 30–50 nm and does not change along the thickness. The crystallites possess relatively perfect crystal structure, which can be seen from the good alignment of smooth lattice fringes in Figure 1b where the middle part of the film is presented.

3.2 Films deposited from high-energy atomic fluxes (low-pressure conditions)

To obtain the films formed from a non-thermalized flux of Cr atoms the depositions were carried out at $P_{\mathrm{Ar}} = 0.2$ Pa on non-heated ($T_s/T_m \approx 0.14$) and heated to 300 °C ($T_s/T_m \approx 0.28$) and 500 °C ($T_s/T_m \approx 0.38$) substrates. Results obtained from detailed investigation of microstructure and crystallographic structure of three different parts of these films can be summarized as follows.

Both of the films deposited on non-heated and heated to 300 °C and 500 °C substrates crystallized only in ordinary HT Cr phase. However, the microstructure and the cell parameter in different parts of these films change along the thickness and the "amplitude" of these changes depend on the growth temperature.

The cell parameter of the film deposited onto non-heated substrate changes between relatively big limits (∼2%), decreasing from the maximal value in the lower film part to smaller values in the middle and upper parts of this film towards the equilibrium value (Tab. 1). The changes in the cell parameter correlate with changes in the film microstructure, which is also non-uniform along the thickness. The lower part of the film consists of small mostly round-shaped crystallites with an average size of about 6–8 nm. The crystal structure of the crystallites is mostly imperfect with a large amount of structural defects. This follows from the presence of poorly aligned, short, often interrupted and not smooth lattice fringes within the crystallites, whose approximate boundaries are denoted with closed dashed lines in Figure 2a. Crystallite size increases and crystal structure improves as the thickness increases. This follows both from direct observation of the microstructure of the upper part of this film and from the SAED pattern taken from this part (insert in Fig. 2b). The average crystallite size in the upper part of this film is about 30–40 nm with crystallites elongated and preferentially oriented along the columns. Temperature measurements similar to those performed for the high-pressure

Table 1. The average lattice parameters of high-temperature (HT) (a) and low-temperature (LT) (a^*) Cr phases measured in different parts of Cr films as a function of the deposition conditions.

Desposition Conditions / Cell Paramater, Å	Non-heated substrate $P_{Ar} = 5$ Pa	Non-heated substrate $P_{Ar} = 0.2$ Pa	$T_s = 300$ °C, $P_{Ar} = 0.2$ Pa	$T_s = 500$ °C, $P_{Ar} = 0.2$ Pa
Upper part	$a^* = 4.592 \pm 0.006$	$a = 2.890 \pm 0.006$	$a = 2.891 \pm 0.007$	$a = 2.891 \pm 0.007$
Middle part	$a^* = 4.585 \pm 0.006$	$a = 2.905 \pm 0.006$	$a = 2.898 \pm 0.012$	$a = 2.890 \pm 0.006$
Lower part	$a^* = 4.583 \pm 0.007$	$a = 2.924 \pm 0.027$	$a = 2.900 \pm 0.007$	$a = 2.890 \pm 0.01$

Note. Lattice parameters of LT phase with primitive cubic lattice and ordinary bcc HT chromium phase are $a^* = 4.588$ [5] and $a = 2.884$ Å [21] correspondently.

conditions have shown that the substrate temperature in this case did not exceed ∼150 °C.

The lattice parameter of the film deposited at T_s = 300 °C changes within smaller limits than that of the film deposited on the non-heated substrate, whereas that deposited at 500 °C does not change along the thickness being a little larger then the equilibrium value (Tab. 1). The microstructure of 500 °C film is also almost uniform along the thickness. The average crystallite size in the lower and upper parts of this film are 20–30 nm and 30–40 nm respectively. Crystallites in the upper part are elongated and preferentially oriented along the columns, whereas those in the lower film part are more equiaxed and distributed more chaotically (Figs. 3a, b). An important feature of this film is that its lattice constant is equal to that of the upper part of the film deposited under the same conditions on non-heated substrate (Tab. 1).

4 Discussion

4.1 Experimental facts

Let us summarize the results. The LT phase forms in the film grown from fully thermalized atoms with minimal influence of the plasma. The microstructure of this film in the most part is uniform along the thickness. At the same time, the film deposited from the flux of non-thermalized atoms and when the plasma radiation is high enough (low-pressure conditions), crystallizes in ordinary bcc HT Cr phase. The microstructure and the lattice parameter of these films are non-uniform along the thickness when the substrate temperature is low. As the temperature increases, the microstructure tends to be uniform and the lattice parameter decreases towards the equilibrium value.

The formation of LT phase indicates that the temperature during the film growth was lower than 400 °C. Weak changes in the cell parameter and in the microstructure in the lower part of this film suggests small increase in the surface temperature as the film growth proceeds and may be a result of the release of the heat of condensation [6,7].

Substrate temperature measurements performed for low-pressure conditions have shown that it was ∼150 °C, which is sufficiently lower than the temperature limit for the existence of the LT phase. However, this film has crystallized in the HT phase without traces of the LT phase. Since the only factor that defines the formation of HT Cr phase is temperature, it is reasonable to assume that the surface temperature developed during the deposition of the film from non-thermalized atoms onto non-heated substrate was at least ≥ 400 °C, at which temperature the formation of the LT phase is impossible. This assumption is supported by the fact that the lattice parameter of the upper part of this film coincides with that of the film deposited at 500 °C (Tab. 1).

Recent confirmation of the existence of high surface temperature during film deposition has been demonstrated using in situ spectroscopic ellipsometry [8,9] that supports earlier results [6,7]. The difference between the simultaneously measured surface and substrate temperatures both for silicon [8] and for diamond [9] films deposited by microwave assisted CVD reaches ∼100 K. Special experiments have shown that the microwave power (MW) does not affect the substrate temperature and the high surface temperature was attributed to the ion bombardment [8]. Actually, it is known that the energetic particles (atoms or ions) impinging on a solid surface produce two major effects, one of which is *thermal* (heating of a solid), and the second is *athermal* (collision-induced effects). At the same time, most of the energy lost by an energetic particle as it stops ends up as heat, and this heat input is far greater than the heat of condensation [10].

A thermal effect produced by a flux of high-energy ions or atoms onto a surface is, to a large degree, similar to that produced by an electron beam. Contemporary theoretical investigations show that the temperature arising in a material subjected to electron beam irradiation is non-uniformly distributed along the sample's thickness, reaching a maximum in the near-surface region (∼100 nm thick), and rapidly decreasing with further penetration of the electrons [11]. The non-uniformly distributed temperature field results in non-uniform structure formation along the sample's thickness. Most radical structure changes undergo in the near-surface region formed from a liquid state [12].

The above reasoning allows us to assume that there exist two different temperatures during the film growth. First is the conventional substrate temperature, whereas the second is the temperature developing within a thin superficial layer on the growth surface.

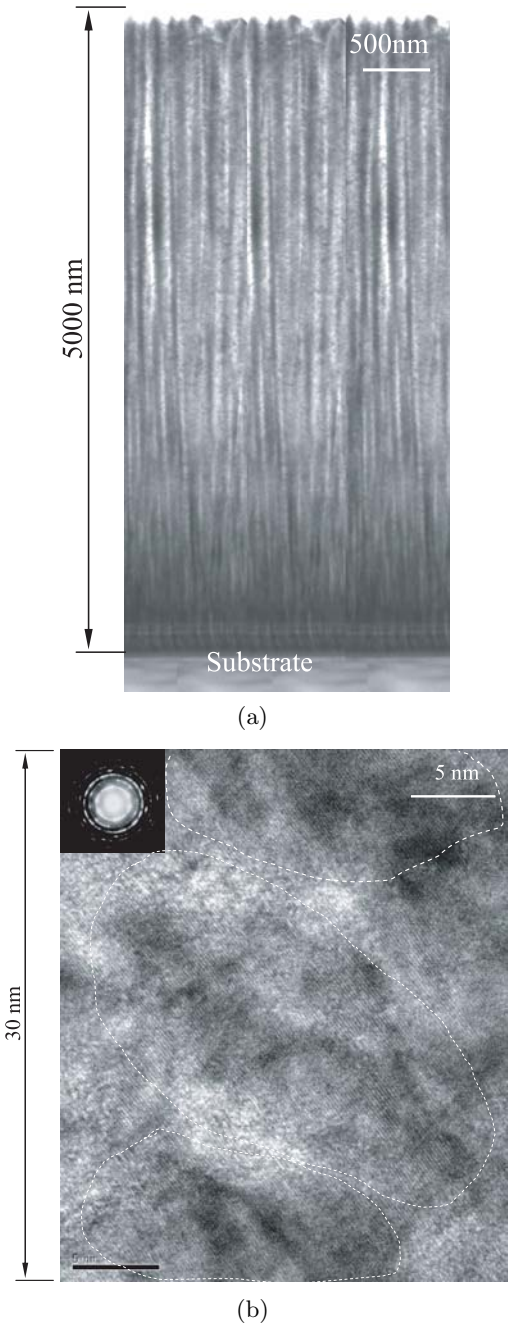

Fig. 1. (a) Cross-sectional view of the film crystallized in low-temperature Cr phase deposited on the backside of non-heated substrate at $P_{\mathrm{Ar}} = 5$ Pa. (b) High-resolution cross-sectional view and the SAED pattern of the middle part of the film presented in (a). Closed dashed lines show the approximate boundaries of the crystallites.

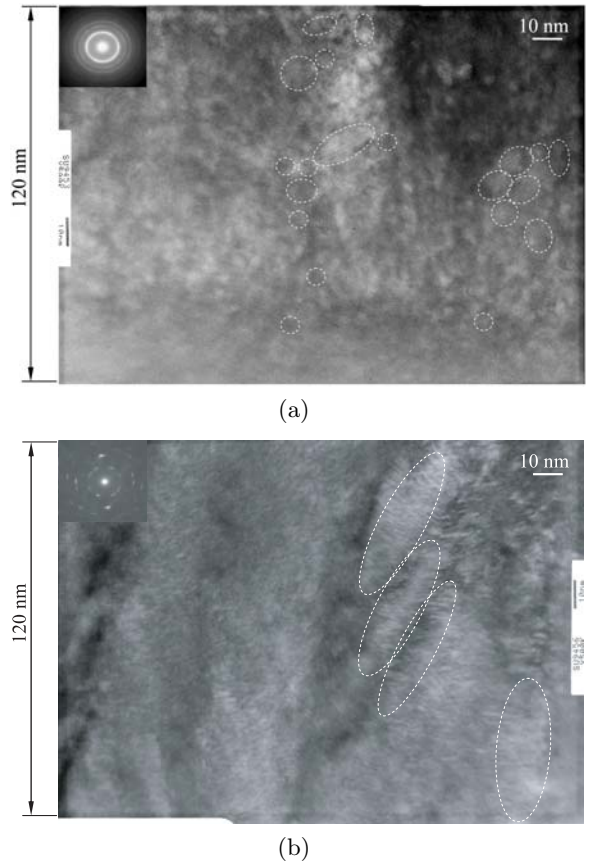

Fig. 2. (a) High-resolution cross-sectional view and the SAED pattern of the lower part of Cr film deposited on non-heated substrate at $P_{\mathrm{Ar}} = 0.2$ Pa. Closed dashed lines show the approximate boundaries of the crystallites. (b) High-resolution cross-sectional view and the SAED pattern of the upper part of Cr film deposited on non-heated substrate at $P_{\mathrm{Ar}} = 0.2$ Pa. Closed dashed lines show the approximate boundaries of the crystallites.

4.2 The "hot layer" model

Basing on our experimental results, we developed a model that explains the appearance of the temperature difference between the growth surface and the substrate during film deposition from high-energy atomic fluxes. The model is based on the supposition of the formation of a thin superficial "hot layer" on a condensation surface during the atomic condensation. The properties of this layer are as follows. (i) The layer consists of mobile (not thermalized) atoms. Clearly, the structure of such a layer is disordered and thus the layer may be considered as a *liquid-like* [13]. (ii) The layer exists during the period of atomic condensation. (iii) The atoms within the layer, which completely dissipated the energy, form a solid film beneath this layer. (iv) The thickness of the layer depends on a flux density and kinetic energy of atoms arriving on a condensation surface and is assumed to be as large as (5–10) atomic layers. Note that the model describes the layer when it has reached its steady state and maximal thickness.

Clearly, the temperature difference between the hot layer and the substrate beneath it can exist in the case of *low thermal conductivity* of this layer. Therefore, at first we will consider the mechanism of a thermal conductivity of the hot layer.

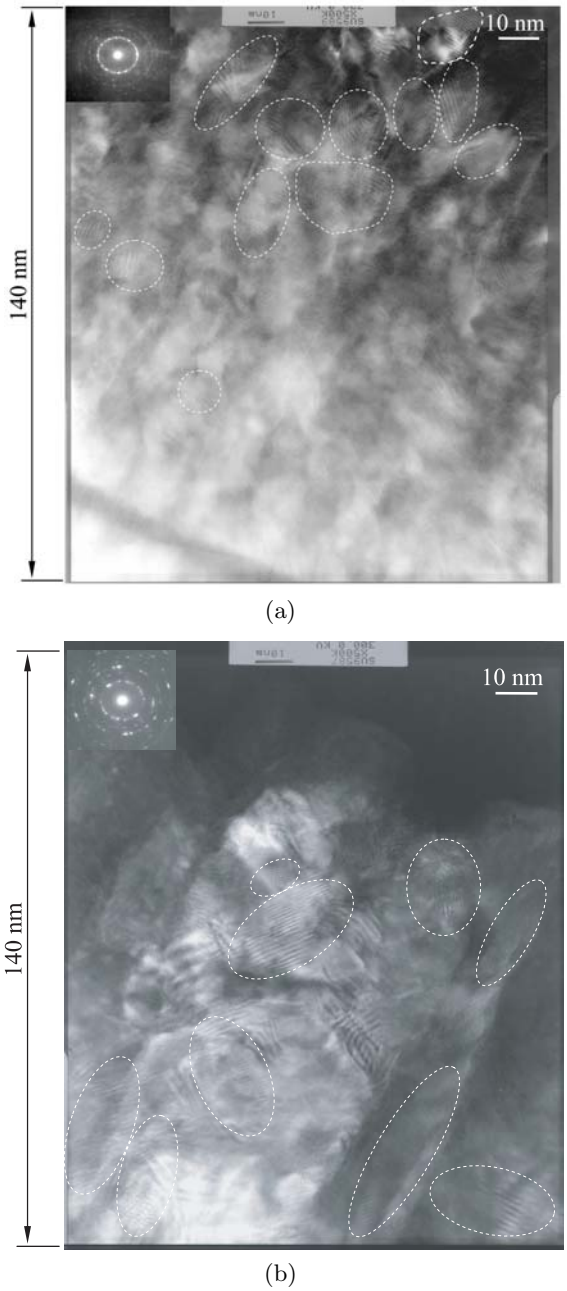

Fig. 3. (a) High-resolution cross-sectional view and the SAED pattern of the lower part of Cr film deposited at $P_{\mathrm{Ar}} = 0.2$ Pa and $T_s = 500$ °C. Closed dashed lines show the approximate boundaries of the crystallites. (b) High-resolution cross-sectional view and the SAED pattern of the upper part of Cr film deposited at $P_{\mathrm{Ar}} = 0.2$ Pa and $T_s = 500$ °C. Closed dashed lines show the approximate boundaries of the crystallites.

Since the atoms in this layer are bound to each other with metallic bonds, we will consider the layer as consisting from two subsystems – the ion subsystem deep in the electron subsystem. Taking into account the liquid-like nature of the hot layer and that the thermal conductivity of liquid metals is provided by the electrons whereas the contribution coming from the phonon thermal conductivity is very low [14], we conclude that the thermal conductivity related to the phonon-like mechanism is strongly limited and is mainly defined by the electron subsystem. The energy exchange between particles within the same subsystem, e.g., between the electrons within the electron subsystem, or between the ions within the ion subsystem is much more efficient and fast than the energy exchange between the ion subsystem and the electron one. The reason for this is a marked difference of the mass of ions and electrons. In fact, if the time τ is needed to transfer the energy δE within the electron subsystem, then the time, which is needed to transfer the same δE energy from the ion subsystem to the electron subsystem, will be $M_a/m_e{\cdot}\tau$ (M_a is the mass of atom) [15], that is much longer then τ.

The energy stored in the hot layer can be found from the following reasoning. The average kinetic energy of ions in the hot layer, E is somewhat less than the energy E_0 of atoms arriving on the condensation surface, because of some dissipation of the energy in the layer. Then the average velocity v_a of ions within the hot layer is $v_a \sim (2E/M_a)^{1/2}$. At the same time, the average velocity v_e of electrons within the hot layer will be approximately $v_e \sim v_a$ because they belong to the condensing atoms before the electron subsystem has formed. Since $M_a \gg m_e$ where m_e is the bare electron mass it is clear that $E_e \sim m_e \cdot v_a^2/2 \ll M_a{\cdot}v_a^2/2$. On the other hand, when electrons join the electron subsystem their energy becomes equal to the energy of the electron system of the solid film due to the fast transport properties of electrons. Thus, it is clear that the main part of the energy stored in a hot layer is stored in the ion subsystem. We can also conclude that only a small part of the energy stored in the hot layer can be transmitted by the electron subsystem to the solid film per time unit.

To transform from the liquid-like state to a solidified one, the ion subsystem of the hot layer has to dissipate its energy. It can be done in different ways: by transferring the energy (i) to the electron subsystem, (ii) to the solid film beneath the hot layer, and (iii) by radiation. As it was shown, the energy exchange between the ion and electron subsystems in the hot layer is strongly depressed. Another possible mechanism of the energy transfer from the hot layer to the solid film beneath is a phonon-like mechanism. However, as it was mentioned, phonon thermal conductivity in liquid (as well as in solid) metals is very low. Thus, in view of a liquid-like nature of a hot layer the phonon-like mechanism of the heat transfer from the layer to the film beneath is of very low importance. The last mechanism of energy dissipation is the emission of radiation by the ion subsystem of the hot layer. Obviously, just this radiation has been recorded during the surface temperature measurements during condensation of evaporated Ag films [16].

Thus, we expect that the hot layer possesses very low thermal conductivity whose value can be estimated as follows.

The thermal conductivity k_e of a metal both in the bulk and film states is mostly determined by electrons and is defined from the conventional kinetic theory by the

well-known equation [13]

$$k_e = \frac{1}{3} v_e \cdot c_e \cdot \lambda_e \tag{1}$$

where c_e is the specific heat, λ_e is the mean free path of electrons, v_e is the average electron velocity. Since in our case the heat is accumulated in the ion subsystem and has to be transferred to the electron subsystem, the thermal conductivity of the hot layer is defined by the ion subsystem. Therefore, to estimate its thermal conductivity k_a we also use equation (1), however, all *parameters related to the electrons* should be *substituted* by the *corresponding parameters related to the ion subsystem*. The thermal conductivity k_a should be multiplied by factor $m_e/M_a \cdot \lambda_a/\lambda_e \cdot v_a/v_e$, where m_e/M_a determines the decrease in the energy transfer from ions to electrons, $\lambda_a/\lambda_e \cdot v_a/v_e$ characterizes the decrease in the thermal conductivity due to both the decrease of the mean free path λ_a of ions and their average velocity v_a. Thus,

$$k_a \cong k_e \frac{m_e}{M_a} \frac{\lambda_a}{\lambda_e} \frac{v_a}{v_e}. \tag{2}$$

For Cr ($M_a \cong$ 50 a.m.u.) $m_e/M_a \cong 10^{-5}$, assuming that $\lambda_a \cong 2$ Å which is equal to the average interatomic distance in a liquid [13] and $\lambda_e \cong 400$ Å [17]), the $\lambda_a/\lambda_e \cong 5\times10^{-3}, v_a/v_e \cong (m_e/M_a)^{1/2} \cong 3\times10^{-3}$. Upon substituting these values in (2) we obtain $k_a \sim 10^{-10} \cdot k_e$. That is, the effective thermal conductivity of the hot layer formed during chromium deposition is ten orders of magnitude lower than the conventional thermal conductivity of bulk chromium. Let us note that k_a varies in limits $10^{-9}-10^{-11}$ when M_a varies in limits 12 (carbon) – 182 (tungsten) amu, i.e., the thermal conductivity of a hot layer is extremely low and only slightly depends on the properties of the depositing element.

To evaluate the temperature T_l of the hot layer one could apply conventional kinetic theory. However, kinetic theory is applicable when the mean free path λ of heat transmitting particles is much larger than the average distance $a$between the particles, $\lambda \gg a$ [13]. In our case, the mean free path of ions in a liquid-like hot layer, $\lambda \sim a$, and application of conventional kinetic theory becomes questionable. Therefore, to estimate the temperature T_l we use the heat diffusion equation and the effective thermal conductivity k_a.

To determine the temperature $T_l(x,t)$ of the hot layer as a function of time t and coordinate x (x is the distance from the film beneath) we apply the one-dimensional heat diffusion equation:

$$\frac{d}{dt}\left(c(x)n(x)T\right) = \frac{d}{dx}\left(k_a(x)\frac{dT_l}{dx}\right). \tag{3}$$

Here $c(x)$ is the specific heat, n is the density, and $k_a(x)$ is the thermal conductivity of the hot layer. For the sake of simplicity, we consider the *steady state conditions* for which all these quantities become functions only of x and equation (3) transforms to

$$\frac{d}{dx}\left(k_a(x)\frac{dT_l}{dx}\right) = 0. \tag{4}$$

The general solution of equation (4) is given by

$$T_l(x) = c_1 \int \frac{dx}{k_a(x)} + c_2. \tag{5}$$

To find the temperature T_l from (5) one should know c_1 and c_2 constants. The constant c_1 can be determined from the condition that at $x = 0$ the heat flux delivered to the top of a hot layer is q and differentiating both parts of (5) with respect to x we obtain

$$(k_a(x)\frac{dT_l}{dx})_{x=0} = -q. \tag{6}$$

Thus, we obtain $c_1 = q$. The constant c_2 is derived from the condition at $x \geq L$ (L is the thickness of a hot layer) where T_l is equal to the substrate temperature T_s

$$T_l(x = L) = q \int \frac{dx}{k_a(x)_{x=L}} + c_2 = T_s. \tag{7}$$

It follows from equation (6) that the thermal gradient at the surface of the hot layer, defined as

$$\frac{dT_l}{dx_{x=0}} = -\frac{q}{k_a(x=0)} \tag{8}$$

can be very large because $k_a(x = 0)$ is small. Now, considering the simplest case when $k_a(x) = k_a$ and substituting k_a, c_1 and c_2 into equation (5), we obtain

$$T_l(x) = \frac{q}{k_a}(L - x) + T_s. \tag{9}$$

The temperature $T_l(x)$ reaches its maximum value T_m on the top of a hot layer, and coincides with T_s at $x = L$:

$$T_m = T_l(x = 0) = \frac{Lq}{k_a} + T_s. \tag{10}$$

It is seen from equation (10) that as the energy flux q delivered to the growth surface by condensing atoms and from the plasma, increases so does the temperature of the hot layer, T_m.

To estimate T_m one should know the liquid-like layer thickness L. In the conditions of our experiments, measurement of the thickness L is impossible. However, taking into account investigations of the effect of the surface melting of In and Pb island films [18,19] we can assume, that it may span 5–10 atomic layers, i.e., $L \sim 1.5$–3 nm. Substituting in equation (10) $q = 0.1$ W/cm^2 calculated for our experimental deposition conditions, remembering that $k_a \sim 10^{-10} \cdot k_e$ and $k_e \cong 100$ W/m K for Cr, we obtain that $T_m \cong$ (150–300 K)+T_s. Despite the fact that the model only allows estimation of the order of magnitude of the surface temperature, the calculated value is close to that obtained in the experiment. Our results show that the surface temperature during Cr deposition on non-heated substrate in low-pressure conditions is about 400–500 °C, whereas the measured substrate temperature does not exceed 150 °C.

Thus, we see that the thin superficial layer existing on the top of a solid film during the film deposition by magnetron sputtering can be noticeably overheated with respect to the film. However, as it was mentioned earlier, the *surface temperature develops gradually* and reaches its maximum when steady-state conditions are established. This means that the structure of the film region adjacent to the substrate forms at relatively low surface temperature whereas that of the upper part grows at higher temperature established at steady state conditions. Therefore, if q is small during the deposition, the surface temperature is close to the substrate temperature and the film structure should be uniform along the thickness. This case is realized for the Cr film deposited from low q in high-pressure conditions (Fig. 1a). Whereas the large value of q (low-pressure low-temperature conditions) results in the formation of non-uniform film structure along the thickness as is seen in Figure 2a, b.

On the other hand, the experiment shows that the film structure improves and becomes uniform when the film is deposited on a heated substrate. This effect is also explained by the model. In fact, when deriving equation (10), we did not take into account the contribution to the flux q coming from the outgoing heat flux due to the radiation from the hot layer. It can be included provided that q is mainly determined by the energy flux delivered by condensing atoms and from the plasma. Obviously, the outgoing flux is to be subtracted from the flux q. It follows from the Stefan-Boltzmann law that the outgoing heat flux grows at least as σT_s^4 because T_m is proportional to T_s as seen from equation (10). Thus, at elevated substrate temperatures T_s, the total flux q is strongly diminished due to the outgoing flux, and T_m tends to T_s, see equation (10). That is, the difference between T_m and T_s, (the temperature gradient during the film growth), reduces with increasing T_s. At a certain temperature of the substrate, T_m will be practically equal to the T_s. This effect is observed for the film deposited at $T_s = 500$ °C. The uniform lattice constant (Tab. 1) and the microstructure (Fig. 3a, b) along the thickness of this film testify to the small temperature gradient developed during the deposition.

Let us note that our preliminary in situ measurements of the surface temperature using VARIOSCAN high resolution thermography system (JENOPTIK Laser, Optik Systeme GmbH) have shown that the surface temperature developed during deposition of the Cr film at low-pressure low-temperature conditions ($q \approx 0.17$ W cm^{-2}) reaches ∼800 °C whereas simultaneously measured substrate temperature does not exceed 250 °C. This result fairly confirms the results presented in this paper.

4.3 The film structure model

From the preceding discussion, it follows that the proposed model adequately explains the experimental data. Thus, it is reasonable to conclude that the main reason for the formation of a non-uniform structure along the thickness observed for sputter-deposited films is the gradual increase of the surface temperature during the film growth. A schematic illustration of such a film structure as a function of the normalized *real* growth temperature, T_{surf}/T_m, where T_{surf} is the surface temperature developing during the film growth, is presented in Figure 4b. For comparison, the micrographs of a real structure of Cr film deposited at low-pressure low-temperature conditions are also presented. The upper limit of $T_{surf}/T_m \approx 0.4$ relates to the experimentally found $T_{surf} \approx 500$ °C in the upper part of Cr film, whereas the lower limit $T_{surf}/T_m \approx 0.14$ relates to the initial condition $T_{surf} = T_s$ at which the lower part of the film formed.

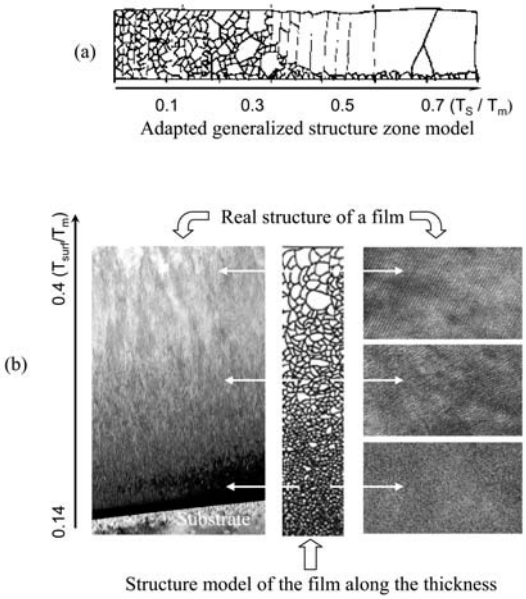

Fig. 4. Film structure zone models: (a) Adapted generalized conventional structure zone model; (b) model of the film structure along the thickness (center), illustrated with: left side – general cross-sectional view of Cr film deposited on non-heated substrate at $P_{\mathrm{Ar}} = 0.2$ Pa; right side – high–resolution cross-sectional views of different parts of this film.

Let us compare our model with known structure zone models [3,20]. In these models, describing the evolution of the film structure, as a function of T_s/T_m, there is no differentiation is made between the surface and substrate temperatures and these parameters do not change during the growth of the film. A generalized illustration of these models composed of a set of discrete film structures forming at certain T_s/T_m values arranged along the normalized growth temperature axis T_s/T_m is shown in Figure 4a. Comparing illustrations of the generalized conventional structure zone model in Figure 4a with the proposed in Figure 4b, one can easily observe, that these models are quite similar. The similarity of schemes is conditioned by the similarity of the growth processes occurring in the film at a certain temperature. However, the difference between the models is that in our model, the surface temperature naturally elevates during the film growth, while conventional models consider the film structure to

be unchangeable along the thickness and deal with discrete film structures forming at certain growth temperatures.

5 Conclusions

Chromium films deposited by magnetron sputtering on non-heated substrates from non-thermalized atoms crystallize in regular bcc Cr phase, have non-uniform microstructure and lattice constant along the thickness. These non-uniformities decrease with elevation of the substrate temperature and vanish at a certain value. At the same time, the films deposited on non-heated substrates from the thermalized atoms crystallize in low-temperature Cr phase and have almost uniform microstructure. We developed a model explaining these effects. The model is based on the assumption that during the condensation of sputtered metal atoms, a liquid-like hot layer consisting of mobile atoms forms on the condensation surface. Calculations show that the effective thermal conductivity of the hot layer is about ten orders of magnitude lower than the conventional thermal conductivity of bulk metals and weakly depends on the atomic mass of sputtered metal. Such low thermal conductivity results in development of high temperature difference between the surface and the substrate, which linearly increases with increasing the energy flux delivered to the growth surface by sputtered atoms and from the plasma, and decreases with increasing substrate temperature. Preliminary measurements of the surface temperature show that it can reach ∼700 °C while the simultaneously measured substrate temperature does not exceed 250 °C. Detailed investigation of the crystal structure and microstructure of Cr films deposited on substrates at various temperatures and energy fluxes delivered to the growing surface, correlate well with the above model.

The authors are grateful for the financial support provided by the Korea Science and Engineering Foundation through the Center for Advanced Plasma Surface Technology (CAPST) at Sungkyunkwan University. The authors also express their gratitude to PhD student N.V. Britun (CAPST) for the deposition and preparation of cross-sections of some samples.

References

1. L. Shaginyan, J-G. Han, H-M. Lee, Jpn J. Appl. Phys. **43** (5A), 2594 (2004)
2. J.A. Thornton, Thin Solid Films **54**, 23 (1978)
3. M. Ohring, *The Materials Science of Thin Films*, 2nd edn. (Academic Press, New York, 2002)
4. K.S. Fancey, Surf. & Coat. Technol. **71**, 16 (1995)
5. K. Kimoto, I. Nishida, J. Phys. Soc. Jpn, **22**, 744 (1967)
6. M.V. Belous, C.M. Wayman, J. Appl. Phys. **38**, 5119 (1967)
7. G. Breitweiser, B.N. Varadarajan, J. Wafer, J. Vac. Sci. Technol. **7**, 274 (1969)
8. D. Daineka, V. Suendo, P.R.I. Cabarrocas, Thin Solid Films **468**, 298 (2004)
9. M. Wakagi, B.G. Hong, H.V. Nguen, R.W. Collins, W. Drawl, R. Messier, J. Vac. Sci. Technol. A **13**(4), 1917 (1995)
10. D.L. Smith, *Thin Film Deposition* (McGraw Hill Book Comp., New York, 1997)
11. D.I. Proskurovsky et al., J. Vac. Sci. Technol. A **16** (4), 2480 (1998)
12. D.I. Proskurovsky et al., Surf. & Coat. Technol. **125**, 49 (2000)
13. D. Tabor, *Gases, Liquids and Solids* (Cambridge University Press, Cambridge, 1991)
14. *Encyclopedia of Physics*, Vol. 2 (in Russ.) (Sovetskaya Encyclopediya, Moskow, 1988)
15. E.M. Lifshitz, L.P. Pitaevskii, *Physical Kinetics* (Butterworth-Heinemann Ltd, Oxford, 2002)
16. E. Yoda, *Proc. 6th Intern. Conf. Electron Microscopy*, Kyoto, 1966, p. 517
17. N.F. Mott, H. Jones, *The Theory of the Properties of Metals and Alloys* (Dover Publications, Inc., New York, 1958)
18. M.K. Zayed, M.S. Hegazy, H.E. Elsayed-Ali, Thin Solid Films, **449**, 254 (2004)
19. K.F. Peters, J.B. Cohen, Y.-W. Chung, Phys. Rev. B **57**, 13430 (1998)
20. I. Petrov, P.B. Barna, L. Hultman, J.E. Greene, J. Vac. Sci. Technol. A **21** (5), S117 (2003)
21. *Smithells Metals Reference Book*, 7th edn., edited by E.A. Brandes, G.B. Brook (Elsevier, G.B., 1998)